Higgs Transverse Momentum with a Jet Veto: A Double-Differential Resummation

Pier Francesco Monni,[1] Luca Rottoli[●],[2] and Paolo Torrielli[●][3]

[1]*CERN, Theoretical Physics Department, CH-1211 Geneva 23, Switzerland*
[2]*Dipartimento di Fisica G. Occhialini, U2, Università degli Studi di Milano-Bicocca and INFN,*
Sezione di Milano-Bicocca, Piazza della Scienza, 3, 20126 Milano, Italy
[3]*Dipartimento di Fisica and Arnold-Regge Center, Università di Torino and INFN, Sezione di Torino,*
Via P. Giuria 1, I-10125 Turin, Italy

We consider the simultaneous measurement of the Higgs (p_t^H) and the leading jet (p_t^J) transverse momentum in hadronic Higgs-boson production, and perform the resummation of the large logarithmic corrections that originate in the limit $p_t^H, p_t^J \ll m_H$ up to next-to-next-to-leading-logarithmic order. This work constitutes the first simultaneous (double differential) resummation for two kinematic observables of which one involves a jet algorithm in hadronic collisions, and provides an important milestone in the theoretical understanding of joint resummations. As an application, we provide precise predictions for the Higgs transverse-momentum distribution with a veto $p_t^J \leq p_t^{J,v}$ on the accompanying jets, whose accurate description is relevant to the Higgs precision programme at the Large Hadron Collider.

DOI: 10.1103/PhysRevLett.124.252001

The thorough scrutiny of the properties of the Higgs boson [1,2] is central to the future physics program of the Large Hadron Collider (LHC). In the high-luminosity run of the LHC, the experimental precision in Higgs-related measurements will increase significantly [3], hence allowing for detailed studies of the Higgs sector of the standard model (SM) Lagrangian.

A full exploitation of such measurements requires an unprecedented level of precision in the theoretical description of the relevant observables. In this context, a prominent role is played by kinematic distributions of the Higgs boson and the accompanying QCD radiation, which are sensitive to potential new-physics effects, such as modifications of light-quark Yukawa couplings [4,5], or heavy new-physics states [6–11]. Experimental analyses of Higgs processes typically categorize the collected events in *jet bins*, according to the different number of jets—collimated bunches of hadrons in the final state—produced in association with the Higgs boson. Since the future performance of the LHC will allow for the precise measurement of kinematic distributions in different jet bins, it is paramount to achieve an accurate theoretical understanding of Higgs observables at the multidifferential level.

In this Letter we consider Higgs-boson production in gluon fusion, the dominant channel at the LHC, and we focus on the Higgs transverse-momentum (p_t^H) spectrum in the presence of a veto $p_t^{J,v}$ bounding the transverse momentum p_t^J of the hardest accompanying jet. Veto constraints of such a kind are customarily enforced to enhance the Higgs signal with respect to its backgrounds, relevant examples being the selection of $H \rightarrow W^+ W^-$ events from $t\bar{t} \rightarrow W^+ W^- b\bar{b}$ production [12,13] or the categorization in terms of different initial states [14].

Fixed-order perturbative predictions of the p_t^H spectrum in gluon fusion are currently available at next-to-next-to-leading order (NNLO) in the strong coupling α_s [15–19] in the infinite top-mass limit, and heavy-quark mass effects are known up to next-to-leading order (NLO) [20–24]. Fixed-order perturbation theory is, however, insufficient to accurately describe the observable considered here. When exclusive cuts on radiation are applied, it is well known that the convergence of the perturbative expansion is spoiled by the presence of logarithms $\ell \in \{\ln(m_H/p_t^H), \ln(m_H/p_t^{J,v})\}$ that become large in the limit $p_t^H, p_t^{J,v} \ll m_H$, where the Higgs mass m_H represents the typical hard scale of the considered process. In this regime, such large logarithmic terms must be summed to all perturbative orders to obtain a reliable theoretical prediction. The resummation accuracy is commonly defined at the level of the logarithm of the cumulative cross section, where terms of order $\alpha_s^n \ell^{n+1}$ are referred to as leading logarithms (LL), $\alpha_s^n \ell^n$ as next-to-leading logarithms (NLL), $\alpha_s^n \ell^{n-1}$ as next-to-next-to-leading logarithms (NNLL), and so on. The resummation of the inclusive p_t^H spectrum has been carried out up to high perturbative accuracy [25–28] and is currently known to N³LL order [29,30]. Such calculations have been combined

with NNLO fixed order in Refs. [29–31] to obtain an accurate prediction across the whole p_t^H spectrum. Similarly, the resummation of the jet-vetoed cross section has been achieved in Refs. [32–38], reaching NNLL accuracy matched to N³LO [39]. Related resummations of the transverse momentum imbalance of the Higgs and the hardest jet have been also considered in Refs. [40–42].

In this work, we present the first *joint* resummation of both classes of logarithms, by obtaining a prediction which is differential in both p_t^H and p_t^J, and NNLL accurate in the limit $p_t^H, p_t^J \ll m_H$. Specifically, we integrate the double-differential distribution $d\sigma/dp_t^J dp_t^H$ over p_t^J up to $p_t^J = p_t^{J,v}$, which results in the single-differential p_t^H distribution with a jet veto. The results presented here are of phenomenological relevance in the context of the Higgs physics program at the LHC, and constitute an important milestone in the theoretical understanding of the structure of resummations of pairs of kinematic observables, which has received increasing interest lately [43–45]. Different kinds of joint resummations for hadronic Higgs production have been considered in the literature. Relevant examples are combined resummations of logarithms of p_t^H and small x [46,47], of p_t^H and large x [48–51], of small x and large x [52], and of $p_t^{J,v}$ and the jet radius [39].

To derive the main result of this Letter, it is instructive to first consider the standard transverse-momentum resummation [53,54], starting with a description of the effects that enter at NLL in a toy model with scale-independent parton densities. The core of the inclusive p_t^H resummation lies in the description of soft, collinear radiation emitted off the initial-state gluons and strongly ordered in angle. Observing that in such kinematic configurations each emission is independent of the others, one obtains the following formula in impact-parameter (b) space:

$$\frac{d\sigma}{d^2\vec{p}_t^H} = \sigma_0 \int \frac{d^2\vec{b}}{4\pi^2} e^{-i\vec{b}\cdot\vec{p}_t^H}$$
$$\times \sum_{n=0}^{\infty} \frac{1}{n!} \prod_{i=1}^{n} \int [dk_i] M^2(k_i)(e^{i\vec{b}\cdot\vec{k}_{t,i}} - 1), \quad (1)$$

where σ_0 denotes the Born cross section, and $[dk_i]M^2(k_i)$ is the phase space and squared amplitude for emitting a parton of momentum k_i. The exponential factor in Eq. (1) encodes in a factorized form the kinematic constraint $\delta^2(\vec{p}_t^H - \sum_{i=1}^{n} \vec{k}_{t,i})$, while the -1 term in the round brackets arises because, by unitarity, virtual corrections come with a weight opposite to that of the real emissions, but do not contribute to p_t^H. The factorization of the phase-space constraint allows for an exact exponentiation of the radiation in Eq. (1), leading to the well-known formula of Refs. [53,54].

In order to include the constraint due to a veto on accompanying jets, let us first consider the effect of a jet algorithm belonging to the k_t-type family (such as the

anti-k_t algorithm [55]). Owing to the strong angular separation between the emissions, the clustering procedure at NLL will assign each emission to a different jet [32]. Therefore, imposing a veto $p_t^{J,v}$ on the resulting jets corresponds to constraining the real radiation with an extra factor

$$\Theta(p_t^{J,v} - \max\{k_{t,1}, ..., k_{t,n}\}) = \prod_{i=1}^{n} \Theta(p_t^{J,v} - k_{t,i}). \quad (2)$$

Plugging the above equation into Eq. (1) leads to

$$\frac{d\sigma(p_t^{J,v})}{d^2\vec{p}_t^H} = \sigma_0 \int \frac{d^2\vec{b}}{4\pi^2} e^{-i\vec{b}\cdot\vec{p}_t^H}$$
$$\times \sum_{n=0}^{\infty} \frac{1}{n!} \prod_{i=1}^{n} \int [dk_i] M^2(k_i)[e^{i\vec{b}\cdot\vec{k}_{t,i}}\Theta(p_t^{J,v} - k_{t,i}) - 1]$$
$$= \sigma_0 \int \frac{d^2\vec{b}}{4\pi^2} e^{-i\vec{b}\cdot\vec{p}_t^H} e^{-S_{\mathrm{NLL}}}, \quad (3)$$

where the radiator S_{NLL} reads [32]

$$S_{\mathrm{NLL}} = -\int [dk] M^2(k)[e^{i\vec{b}\cdot\vec{k}_t}\Theta(p_t^{J,v} - k_t) - 1]. \quad (4)$$

To evaluate the above integral, we can perform the integration over the rapidity of the radiation k and obtain

$$\int [dk] M^2(k) = \int \frac{dk_t}{k_t} \frac{d\phi}{2\pi} R'_{\mathrm{NLL}}(k_t), \quad (5)$$

with

$$R'_{\mathrm{NLL}}(k_t) = 4\left(\frac{\alpha_s^{\mathrm{CMW}}(k_t)}{\pi} C_A \ln\frac{m_H}{k_t} - \alpha_s(k_t)\beta_0\right),$$

where β_0 is the first coefficient of the QCD beta function. The coupling in the CMW scheme is defined as [56–58] $\alpha_s^{\mathrm{CMW}}(k_t) = \alpha_s(k_t)\{1 + [(\alpha_s(k_t))/2\pi][([67/18] - [\pi^2/6])C_A - (5/9)n_f]\}$, and includes the contribution of nonplanar soft radiation necessary for NLL accuracy in processes with two hard emitters. The azimuthal integral of Eq. (4) leads to

$$S_{\mathrm{NLL}} = -\int_0^{m_H} \frac{dk_t}{k_t} R'_{\mathrm{NLL}}(k_t)[J_0(bk_t) - 1]$$
$$+ \int_0^{m_H} \frac{dk_t}{k_t} R'_{\mathrm{NLL}}(k_t) J_0(bk_t)\Theta(k_t - p_t^{J,v}). \quad (6)$$

In the first integral, we exploit the large-b property [29,34]

$$J_0(bk_t) \simeq 1 - \Theta(k_t - b_0/b) + \mathcal{O}(\mathrm{N}^3\mathrm{LL}), \quad (7)$$

with $b_0 = 2e^{-\gamma_E}$, to recast Eq. (6) as

$$S_{\text{NLL}} = -Lg_1(\alpha_s L) - g_2(\alpha_s L)$$
$$+ \int_0^{m_H} \frac{dk_t}{k_t} R'_{\text{NLL}}(k_t) J_0(bk_t) \Theta(k_t - p_t^{J,v}), \quad (8)$$

where $\alpha_s \equiv \alpha_s(\mu_R)$ (with μ_R being the renormalization scale), $L = \ln(m_H b/b_0)$, and the g_i functions are those used in the standard p_t^H resummation [59].

The procedure that led to Eq. (3) can be used to extend the above result to higher logarithmic orders. The crucial observation is that, as already stressed, in impact-parameter space the measurement function for p_t^H is entirely factorized, resulting in a phase factor $e^{i\vec{b}\cdot\vec{k}_t}$ for each emission k. This implies that the jet-veto constraint $\Theta(p_t^{J,v} - p_t^J)$ can be included by implementing the jet-veto resummation [34] at the level of the b-space integrand, namely, directly in impact-parameter space. We note incidentally that this observation can be applied to the resummation of other pairs of observables for which the measurement function can be factorized.

We now derive the NNLL result. Starting from Eq. (3), the first step is to promote the $R'_{\text{NLL}}(k_t)$ function that appears in the radiator S_{NLL} to NNLL. The corresponding expression is given in Refs. [29,34], and leads to

$$S_{\text{NNLL}} \equiv -Lg_1(\alpha_s L) - g_2(\alpha_s L) - \frac{\alpha_s}{\pi} g_3(\alpha_s L)$$
$$+ \int_0^{m_H} \frac{dk_t}{k_t} R'_{\text{NNLL}}(k_t) J_0(bk_t) \Theta(k_t - p_t^{J,v}). \quad (9)$$

The above step assumes that the veto on the radiation is encoded in a phase-space constraint of the type (2). While this approximation is correct at NLL, where the jet algorithm does not recombine the emissions with one another, it fails beyond this order. Specifically, up to NNLL, at most two soft emissions can become close in angle (three unordered soft emissions only contribute to N³LL), and therefore may get clustered into the same jet (whose momentum is defined according to the so-called E scheme, where the four momenta of the constituents are added together). The configurations in which the resulting cluster is the leading jet are not correctly described by the constraint in Eq. (2). In order to account for this effect, one has to include a *clustering* correction [34] in impact parameter space, that reads

$$\mathcal{F}_{\text{clust}} = \frac{1}{2!} \int [dk_a][dk_b] M^2(k_a) M^2(k_b) J_{ab}(R) e^{i\vec{b}\cdot\vec{k}_{t,ab}}$$
$$\times [\Theta(p_t^{J,v} - k_{t,ab}) - \Theta(p_t^{J,v} - \max\{k_{t,a}, k_{t,b}\})], \quad (10)$$

where $\vec{k}_{t,ab} = \vec{k}_{t,a} + \vec{k}_{t,b}$ and $k_{t,ab}$ is its magnitude. The constraint $J_{ab}(R) = \Theta(R^2 - \Delta\eta_{ab}^2 - \Delta\phi_{ab}^2)$ restricts the phase space to the region where the recombination between

the two emissions takes place. Here R is the jet radius and $\Delta\eta_{ab}$ and $\Delta\phi_{ab}$ are the pseudorapidity and azimuthal separation between the two emissions, respectively. We observe that Eq. (10) differs from the corresponding clustering correction for the standard jet-veto resummation [34] by the factor $e^{i\vec{b}\cdot\vec{k}_{t,ab}}$, which accounts for the p_t^H constraint in impact-parameter space.

Equation (10) describes the clustering correction due to two independent soft emissions. A similar correction arises when the two soft emissions k_a, k_b are correlated, i.e., their squared matrix element cannot be factorized into the product of two independent squared amplitudes. The contribution of a pair of correlated emissions is accounted for in the CMW scheme for the strong coupling that was already used in the NLL radiator (4). However, such a scheme is obtained by integrating *inclusively* over the correlated squared amplitude $\tilde{M}^2(k_a, k_b)$, given in Ref. [63]. While this inclusive treatment is accurate at NLL, at NNLL one needs to correct for configurations in which the two correlated emissions are not clustered together by the jet algorithm. This amounts to including a *correlated* correction [34] of the form

$$\mathcal{F}_{\text{correl}} = \frac{1}{2!} \int [dk_a][dk_b] \tilde{M}^2(k_a, k_b)[1 - J_{ab}(R)] e^{i\vec{b}\cdot\vec{k}_{t,ab}}$$
$$\times [\Theta(p_t^{J,v} - \max\{k_{t,a}, k_{t,b}\}) - \Theta(p_t^{J,v} - k_{t,ab})]. \quad (11)$$

The corrections (10) and (11) describe the aforementioned effects for a single pair of emissions. At NNLL, all remaining emissions can be considered to be far in angle from the pair k_a, k_b, and therefore they never get clustered with the jets resulting from Eqs. (10) and (11).

As a final step towards a NNLL prediction, one must account for non-soft collinear emissions off the initial-state particles. Since a k_t-type jet algorithm never clusters the soft emissions discussed above with non-soft collinear radiation, the latter can be conveniently handled by taking a Mellin transform of the resummed cross section. In Mellin space, the collinear radiation gives rise to the scale evolution of the parton densities $f(\mu)$ and of the collinear coefficient functions $C(\alpha_s)$. The latter, as well as the hard-virtual corrections $\mathcal{H}(\alpha_s)$, must be included at the one-loop level for a NNLL resummation. The equivalent of the clustering and correlated corrections for hard-collinear radiation enters only at N³LL, and therefore is neglected in the following.

After applying to hard-collinear emissions the same procedure detailed above for soft radiation, we obtain the main result of this Letter, namely, the NNLL master formula for the p_t^H spectrum with a jet veto $p_t^{J,v}$, differential in the Higgs rapidity y^H:

$$\frac{d\sigma(p_t^{J,v})}{dy^H d^2\vec{p}_t^H} = M_{\text{gg}\to H}^2 \mathcal{H}[\alpha_s(m_H)] \int_{\mathcal{C}_1} \frac{d\nu_1}{2\pi i} \int_{\mathcal{C}_2} \frac{d\nu_2}{2\pi i} x_1^{-\nu_1} x_2^{-\nu_2} \int \frac{d^2\vec{b}}{4\pi^2} e^{-i\vec{b}\cdot\vec{p}_t^H} e^{-S_{\text{NNLL}}} \left(1 + \mathcal{F}_{\text{clust}} + \mathcal{F}_{\text{correl}}\right)$$

$$\times f_{\nu_1,a_1}(b_0/b) f_{\nu_2,a_2}(b_0/b) \left[\mathcal{P}e^{-\int_{p_t^{J,v}}^{m_H} \frac{d\mu}{\mu} \Gamma_{\nu_1}[\alpha_s(\mu)] J_0(b\mu)}\right]_{c_1 a_1} \left[\mathcal{P}e^{-\int_{p_t^{J,v}}^{m_H} \frac{d\mu}{\mu} \Gamma_{\nu_2}[\alpha_s(\mu)] J_0(b\mu)}\right]_{c_2 a_2}$$

$$\times C_{\nu_1,gb_1}[\alpha_s(b_0/b)] C_{\nu_2,gb_2}[\alpha_s(b_0/b)] \left[\mathcal{P}e^{-\int_{p_t^{J,v}}^{m_H} \frac{d\mu}{\mu} \Gamma_{\nu_1}^{(C)}[\alpha_s(\mu)] J_0(b\mu)}\right]_{c_1 b_1} \left[\mathcal{P}e^{-\int_{p_t^{J,v}}^{m_H} \frac{d\mu}{\mu} \Gamma_{\nu_2}^{(C)}[\alpha_s(\mu)] J_0(b\mu)}\right]_{c_2 b_2}, \quad (12)$$

where $x_{1,2} = m_H/\sqrt{s}\, e^{\pm y^H}$, and $M_{\text{gg}\to H}$ is the Born matrix element. The ν_ℓ subscripts denote the Mellin transform, while the latin letters represent flavor indices, and the sum over repeated indices is understood. Here $\mathbf{\Gamma}_{\nu_\ell}$ and $\mathbf{\Gamma}_{\nu_\ell}^{(C)}$ are the anomalous dimensions describing the scale evolution of the parton densities and coefficient functions, respectively. The contours $\mathcal{C}_1$ and $\mathcal{C}_2$ lie parallel to the imaginary axis to the right of all singularities of the integrand. The path-ordering symbol $\mathcal{P}$ has a formal meaning, and encodes the fact that the evolution operators are matrices in flavor space. All the ingredients of Eq. (12) are given in Ref. [59]. The multidifferential distribution $d\sigma/dp_t^J dy^H d^2\vec{p}_t^H$ is simply obtained by taking the derivative of Eq. (12) in $p_t^{J,v}$.

All integrals entering the above formula are finite in four dimensions and can be evaluated numerically to very high precision. We point out that, similarly to the standard p_t^H resummation [28,29], the result in Eq. (12) can also be deduced directly in momentum space, without resorting to an impact-parameter formulation. The momentum-space approach is particularly convenient for computational purposes, in that it gives access to differential information on the QCD radiation, thereby enabling an efficient Monte Carlo calculation. Therefore, we adopt the latter method for a practical implementation of Eq. (12). The relevant formulas are detailed in Ref. [59], and implemented in the RADISH program.

For the numerical results presented below, we choose $\sqrt{s} = 13$ TeV and we adopt the NNPDF3.1 set [64] of parton densities (PDFs) at NNLO, with $\alpha_s(M_Z) = 0.118$. The evolution of the PDFs is performed with the LHAPDF [65] package and all convolutions are handled with HOPPET [66]. We set the renormalization and factorization scale to $\mu_R = \mu_F = m_H = 125$ GeV, and $R = 0.4$. Figure 1 shows Eq. (12) integrated over the rapidity of the Higgs boson y^H and over the $\vec{p}_t^H$ azimuth, as a function of p_t^H and $p_t^{J,v}$. We observe the typical peaked structure along the p_t^H direction, as well as the Sudakov suppression at small $p_t^{J,v}$. The two-dimensional distribution also features a Sudakov shoulder along the diagonal $p_t^H \sim p_t^{J,v}$, which originates from the sensitivity of the differential spectrum to soft radiation in this region beyond leading order [67]. Equation (12) provides a resummation of the logarithms associated with the shoulder in the regime $p_t^H \sim p_t^{J,v} \ll m_H$, which can be appreciated by the absence of an integrable singularity in this region.

To verify the correctness of Eq. (12), we perform a number of checks. As a first observation, we note that in the region $p_t^{J,v} \gtrsim m_H$, the terms $\mathcal{F}_{\text{clust}}$ and $\mathcal{F}_{\text{correl}}$ vanish by construction and, as expected, one recovers the NNLL resummation for the inclusive p_t^H spectrum. Conversely, considering the limit $p_t^H \gtrsim m_H$ (i.e., small b), Eq. (12) reproduces the standard NNLL jet-veto resummation of Ref. [34] as detailed in Ref. [59]. As a further test, we expand Eq. (12) to second order in α_s relative to the Born, and compare the result with an $\mathcal{O}(\alpha_s^2)$ fixed-order calculation for the inclusive production of a Higgs boson plus one jet [68–70], with jets defined according to the anti-k_t algorithm [55]. In particular, to avoid the perturbative instability associated with the Sudakov shoulder, we calculate the double cumulant

$$\sigma(p_t^{J,v}, p_t^{H,v}) \equiv \int dy^H d^2\vec{p}_t^H \frac{d\sigma(p_t^{J,v})}{dy^H d^2\vec{p}_t^H} \Theta(p_t^{H,v} - |\vec{p}_t^H|),$$

and define the quantity

$$\Delta(p_t^{J,v}, p_t^{H,v}) = \sigma^{\text{NNLO}}(p_t^{J,v}, p_t^{H,v}) - \sigma_{\text{exp}}^{\text{NNLL}}(p_t^{J,v}, p_t^{H,v}),$$

where $\sigma^{\text{NNLO}}(p_t^{J,v}, p_t^{H,v})$ is computed by taking the difference between the NNLO total Higgs-production cross section [71–73], obtained with the ggHiggs program [74], and the NLO Higgs + jet cross section for
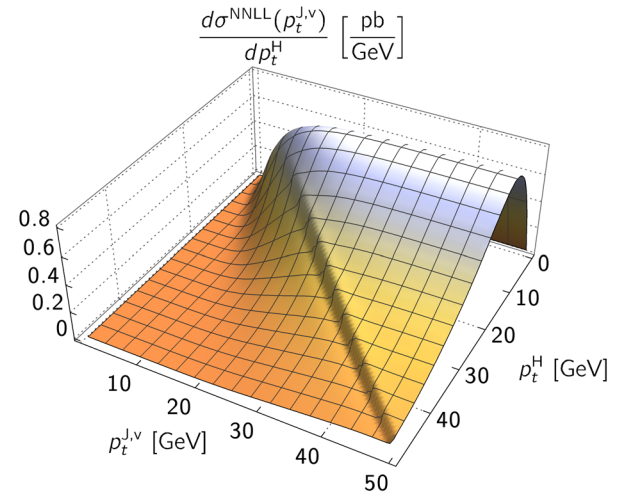

FIG. 1. The NNLL differential distribution (12), integrated over the Higgs-boson rapidity y^H and over the $\vec{p}_t^H$ azimuth, as a function of p_t^H and $p_t^{J,v}$.
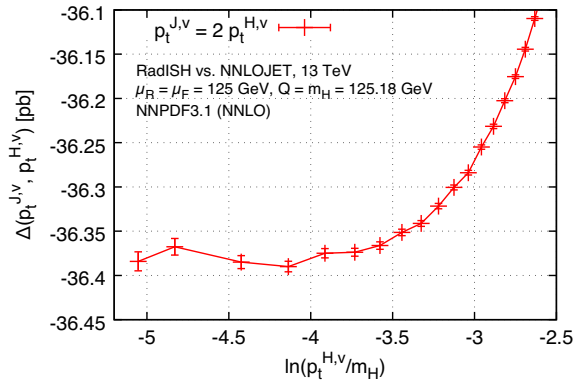
FIG. 2. $\Delta(p_t^{J,v}, p_t^{H,v})$, as defined in the text, at second order in α_s as a function of $\ln(p_t^{H,v}/m_H)$, for $p_t^{J,v} = 2p_t^{H,v}$. This test features a slightly different Higgs mass, $m_H = 125.18$ GeV.

FIG. 3. Matched NNLL + NLO (red band), NLL + LO (blue band), and fixed-order NLO (green band) p_t^H differential distributions for $p_t^{J,v} = 30$ GeV, with theoretical uncertainties estimated as explained in the main text.

$(p_t^J > p_t^{J,v}) \vee (p_t^H > p_t^{H,v})$, calculated with the NNLOJET program [18]. Given that the NNLL prediction controls all divergent terms at the second perturbative order, one expects the quantity Δ to approach a constant value of N³LL nature in the $p_t^H \to 0$ limit. Figure 2 displays this limit for $p_t^{J,v} = 2p_t^{H,v}$, which shows an excellent convergence towards a constant, thereby providing a robust test of Eq. (12).

As a phenomenological application of our result, we set $p_t^{J,v} = 30$ GeV in accordance with the LHC experiments. While Eq. (12) provides an accurate description of the spectrum in the small-p_t^H region, in order to reliably extend the prediction to larger p_t^H values one needs to match the resummed formula to a fixed-order calculation, in which the hard radiation is correctly accounted for. We thus match the NNLL result to the NLO Higgs + jet p_t^H distribution obtained with the program MCFM-8.3 [75,76] by means of the multiplicative matching formulated in Refs. [23,31,77]. We adopt the setup outlined above, and in addition we introduce the resummation scale Q as detailed in the Supplemental Material [59] as a mean to assess the uncertainties due to missing higher logarithmic corrections. To estimate the theoretical uncertainty of our final prediction, we perform a variation of the renormalization and factorization scales by a factor of 2 about the central value $\mu_R = \mu_F = m_H$, while keeping $1/2 \leq \mu_R/\mu_F \leq 2$. Moreover, for central μ_R and μ_F scales, we vary the resummation scale by a factor of 2 around $Q = m_H/2$, and take the envelope of all the above variations. Figure 3 compares the NNLL + NLO prediction to the NLL + LO, and to the fixed-order NLO result. The integral of the NNLL + NLO (NLL + LO) distribution yields the corresponding jet-vetoed cross section at NNLL + NNLO (NLL + NLO) [34].

We observe a good perturbative convergence for the resummed predictions to the left of the peak, where logarithmic corrections dominate. Above $p_t^H \sim 10$ GeV, the NNLL + NLO prediction differs from the NLL + LO
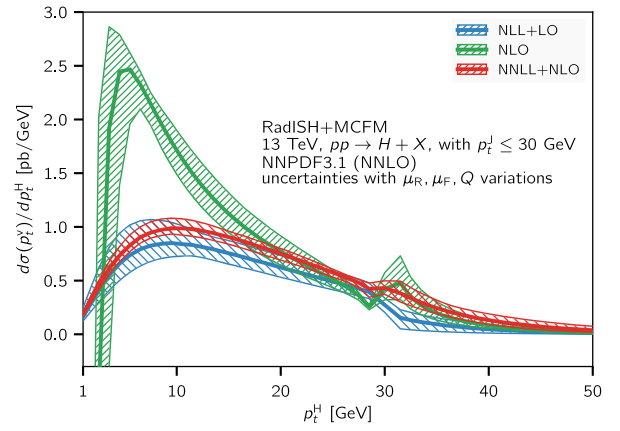
due to the large NLO K factor in the considered process. The residual perturbative uncertainty in the NNLL + NLO distribution is of $\mathcal{O}(10\%)$ for $p_t^H \lesssim p_t^{J,v}$. The comparison to the NLO fixed order shows the importance of resummation across the whole p_t^H region, and a much reduced sensitivity to the Sudakov shoulder at $p_t^H \sim p_t^{J,v}$ (in Fig. 3 we use a 2 GeV bin across the shoulder).

In this Letter we have formulated the first double-differential resummation for an observable defined through a jet algorithm in hadronic collisions. As a case study, we considered the production of a Higgs boson in gluon fusion with transverse momentum p_t^H in association with jets satisfying the veto requirement $p_t^J \leq p_t^{J,v}$. In the limit $p_t^H, p_t^{J,v} \ll m_H$, we performed the resummation of the large logarithms $\ln(m_H/p_t^H), \ln(m_H/p_t^{J,v})$ up to NNLL, resulting in an accurate theoretical prediction for this physical observable. As a phenomenological application, we presented matched NNLL + NLO results at the LHC. Our formulation can be applied to the production of any color-singlet system, and it is relevant in a number of phenomenological applications that will be explored in future work.

[1] G. Aad *et al.* (ATLAS Collaboration), Phys. Lett. B **716**, 1 (2012).

[2] S. Chatrchyan *et al.* (CMS Collaboration), Phys. Lett. B **716**, 30 (2012).

[3] M. Cepeda *et al.* (HL/HE WG2 Group), CERN Yellow Rep. Monogr. **7**, 221 (2019).

[4] F. Bishara, U. Haisch, P. F. Monni, and E. Re, Phys. Rev. Lett. **118**, 121801 (2017).

[5] Y. Soreq, H. X. Zhu, and J. Zupan, J. High Energy Phys. 12 (2016) 045.

[6] A. Banfi, A. Martin, and V. Sanz, J. High Energy Phys. 08 (2014) 053.

[7] C. Grojean, E. Salvioni, M. Schlaffer, and A. Weiler, J. High Energy Phys. 05 (2014) 022.

[8] M. Schlaffer, M. Spannowsky, M. Takeuchi, A. Weiler, and C. Wymant, Eur. Phys. J. C **74**, 3120 (2014).

[9] M. Grazzini, A. Ilnicka, M. Spira, and M. Wiesemann, J. High Energy Phys. 03 (**2017**) 115.

[10] A. Banfi, A. Bond, A. Martin, and V. Sanz, J. High Energy Phys. 11 (2018) 171.

[11] A. Banfi, B. M. Dillon, W. Ketaiam, and S. Kvedaraite, J. High Energy Phys. 01 (**2020**) 089.

[12] M. Aaboud *et al.* (ATLAS Collaboration), Phys. Lett. B **789**, 508 (2019).

[13] A. M. Sirunyan *et al.* (CMS Collaboration), Phys. Lett. B **791**, 96 (2019).

[14] M. Aaboud *et al.* (ATLAS Collaboration), Phys. Rev. D **98**, 052005 (2018).

[15] R. Boughezal, F. Caola, K. Melnikov, F. Petriello, and M. Schulze, Phys. Rev. Lett. **115**, 082003 (2015).

[16] R. Boughezal, C. Focke, W. Giele, X. Liu, and F. Petriello, Phys. Lett. B **748**, 5 (2015).

[17] F. Caola, K. Melnikov, and M. Schulze, Phys. Rev. D **92**, 074032 (2015).

[18] X. Chen, J. Cruz-Martinez, T. Gehrmann, E. W. N. Glover, and M. Jaquier, J. High Energy Phys. 10 (2016) 066.

[19] J. M. Campbell, R. K. Ellis, and S. Seth, J. High Energy Phys. 10 (2019) 136.

[20] J. M. Lindert, K. Melnikov, L. Tancredi, and C. Wever, Phys. Rev. Lett. **118**, 252002 (2017).

[21] J. M. Lindert, K. Kudashkin, K. Melnikov, and C. Wever, Phys. Lett. B **782**, 210 (2018).

[22] S. P. Jones, M. Kerner, and G. Luisoni, Phys. Rev. Lett. **120**, 162001 (2018).

[23] F. Caola, J. M. Lindert, K. Melnikov, P. F. Monni, L. Tancredi, and C. Wever, J. High Energy Phys. 09 (2018) 035.

[24] T. Neumann, J. Phys. Commun. **2**, 095017 (2018).

[25] G. Bozzi, S. Catani, D. de Florian, and M. Grazzini, Nucl. Phys. **B737**, 73 (2006).

[26] T. Becher, M. Neubert, and D. Wilhelm, J. High Energy Phys. 05 (2013) 110.

[27] D. Neill, I. Z. Rothstein, and V. Vaidya, J. High Energy Phys. 12 (2015) 097.

[28] P. F. Monni, E. Re, and P. Torrielli, Phys. Rev. Lett. **116**, 242001 (2016).

[29] W. Bizoń, P. F. Monni, E. Re, L. Rottoli, and P. Torrielli, J. High Energy Phys. 02 (2018) 108.

[30] X. Chen, T. Gehrmann, N. Glover, A. Huss, Y. Li, D. Neill, M. Schulze, I. W. Stewart, and H. X. Zhu, Phys. Lett. B **788**, 425 (2019).

[31] W. Bizoń, X. Chen, A. Gehrmann-De Ridder, T. Gehrmann, N. Glover, A. Huss, P. F. Monni, E. Re, L. Rottoli, and P. Torrielli, J. High Energy Phys. 12 (2018) 132.

[32] A. Banfi, G. P. Salam, and G. Zanderighi, J. High Energy Phys. 06 (2012) 159.

[33] T. Becher and M. Neubert, J. High Energy Phys. 07 (2012) 108.

[34] A. Banfi, P. F. Monni, G. P. Salam, and G. Zanderighi, Phys. Rev. Lett. **109**, 202001 (2012).

[35] T. Becher, M. Neubert, and L. Rothen, J. High Energy Phys. 10 (2013) 125.

[36] I. W. Stewart, F. J. Tackmann, J. R. Walsh, and S. Zuberi, Phys. Rev. D **89**, 054001 (2014).

[37] A. Banfi, P. F. Monni, and G. Zanderighi, J. High Energy Phys. 01 (2014) 097.

[38] J. K. L. Michel, P. Pietrulewicz, and F. J. Tackmann, J. High Energy Phys. 04 (2019) 142.

[39] A. Banfi, F. Caola, F. A. Dreyer, P. F. Monni, G. P. Salam, G. Zanderighi, and F. Dulat, J. High Energy Phys. 04 (2016) 049.

[40] P. Sun, C.-P. Yuan, and F. Yuan, Phys. Rev. Lett. **114**, 202001 (2015).

[41] Y. T. Chien, D. Y. Shao, and B. Wu, J. High Energy Phys. 11 (2019) 025.

[42] P. Sun, J. Isaacson, C.-P. Yuan, and F. Yuan, Phys. Lett. B **769**, 57 (2017).

[43] A. J. Larkoski, I. Moult, and D. Neill, J. High Energy Phys. 09 (2014) 046.

[44] M. Procura, W. J. Waalewijn, and L. Zeune, J. High Energy Phys. 10 (2018) 098.

[45] G. Lustermans, J. K. L. Michel, F. J. Tackmann, and W. J. Waalewijn, J. High Energy Phys. 03 (2019) 124.

[46] S. Marzani, Phys. Rev. D **93**, 054047 (2016).

[47] S. Forte and C. Muselli, J. High Energy Phys. 03 (2016) 122.

[48] E. Laenen, G. F. Sterman, and W. Vogelsang, Phys. Rev. D **63**, 114018 (2001).

[49] A. Kulesza, G. F. Sterman, and W. Vogelsang, Phys. Rev. D **69**, 014012 (2004).

[50] G. Lustermans, W. J. Waalewijn, and L. Zeune, Phys. Lett. B **762**, 447 (2016).

[51] C. Muselli, S. Forte, and G. Ridolfi, J. High Energy Phys. 03 (2017) 106.

[52] M. Bonvini and S. Marzani, Phys. Rev. Lett. **120**, 202003 (2018).

[53] G. Parisi and R. Petronzio, Nucl. Phys. **B154**, 427 (1979).

[54] J. C. Collins, D. E. Soper, and G. F. Sterman, Nucl. Phys. **B250**, 199 (1985).

[55] M. Cacciari, G. P. Salam, and G. Soyez, J. High Energy Phys. 04 (2008) 063.

[56] S. Catani, B. R. Webber, and G. Marchesini, Nucl. Phys. **B349**, 635 (1991).

[57] A. Banfi, B. K. El-Menoufi, and P. F. Monni, J. High Energy Phys. 01 (2019) 083.

[58] S. Catani, D. De Florian, and M. Grazzini, Eur. Phys. J. C **79**, 685 (2019).

[59] See Supplemental Material at http://link.aps.org/supplemental/10.1103/PhysRevLett.124.252001 for additional details on the results of the Letter, including Refs. [60–62].

[60] D. de Florian and M. Grazzini, Nucl. Phys. **B616**, 247 (2001).

[61] T. Becher and M. Neubert, Eur. Phys. J. C **71**, 1665 (2011).

[62] R. K. Ellis, W. J. Stirling, and B. R. Webber, *QCD and Collider Physics* (Cambridge University Press, Cambridge, England, 1996), https://doi.org/10.1017/CBO9780511628788.

[63] Y. L. Dokshitzer, A. Lucenti, G. Marchesini, and G. P. Salam, Nucl. Phys. **B511** (1998) 396; **B593**, 729 (2001).

[64] R. D. Ball *et al.* (NNPDF Collaboration), Eur. Phys. J. C **77**, 663 (2017).

[65] A. Buckley, J. Ferrando, S. Lloyd, K. Nordström, B. Page, M. Rüfenacht, M. Schönherr, and G. Watt, Eur. Phys. J. C **75**, 132 (2015).

[66] G. P. Salam and J. Rojo, Comput. Phys. Commun. **180**, 120 (2009).

[67] S. Catani and B. R. Webber, J. High Energy Phys. 10 (1997) 005.

[68] D. de Florian, M. Grazzini, and Z. Kunszt, Phys. Rev. Lett. **82**, 5209 (1999).

[69] V. Ravindran, J. Smith, and W. L. Van Neerven, Nucl. Phys. **B634**, 247 (2002).

[70] C. J. Glosser and C. R. Schmidt, J. High Energy Phys. 12 (2002) 016.

[71] R. V. Harlander and W. B. Kilgore, Phys. Rev. Lett. **88**, 201801 (2002).

[72] C. Anastasiou and K. Melnikov, Nucl. Phys. **B646**, 220 (2002).

[73] V. Ravindran, J. Smith, and W. L. van Neerven, Nucl. Phys. **B665**, 325 (2003).

[74] R. D. Ball, M. Bonvini, S. Forte, S. Marzani, and G. Ridolfi, Nucl. Phys. **B874**, 746 (2013).

[75] J. M. Campbell, R. K. Ellis, and W. T. Giele, Eur. Phys. J. C **75**, 246 (2015).

[76] R. Boughezal, J. M. Campbell, R. K. Ellis, C. Focke, W. Giele, X. Liu, F. Petriello, and C. Williams, Eur. Phys. J. C **77**, 7 (2017).

[77] W. Bizoń, A. Gehrmann-De Ridder, T. Gehrmann, N. Glover, A. Huss, P. F. Monni, E. Re, L. Rottoli, and D. Walker, arXiv:1905.05171.

SUPPLEMENTAL MATERIAL TO "HIGGS TRANSVERSE-MOMENTUM RESUMMATION WITH A JET VETO" BY PIER FRANCESCO MONNI, LUCA ROTTOLI, PAOLO TORRIELLI

We here provide supplemental formulae that complete the discussions and results of the letter.

1. Explicit resummation formulae

In the present section we report the explicit expressions for the resummation functions g_1, g_2 and g_3 computed in [25]. We report the results after the introduction of a resummation scale Q, as described in [25,34], that allows for an assessment of the size of subleading logarithmic corrections. With this convention, and a slight abuse of notation, we redefine $L = \ln(Qb/b_0)$, and $\lambda = \alpha_s\beta_0 L$. Here α_s denotes $\alpha_s(\mu_{\rm R})$, Q is the resummation scale, of the order of the hard scale $m_{\rm H}$, while $\mu_{\rm R}$ and $\mu_{\rm F}$ denote the renormalisation and factorisation scales, respectively. The Sudakov radiator S then reads (the formulae in the letter correspond to setting $Q = m_{\rm H}$)

$$S_{\rm N(N)LL} \equiv R_{\rm N(N)LL}(L) + \int_0^Q \frac{dk_t}{k_t} R'_{\rm N(N)LL}(k_t) J_0(bk_t)\Theta(k_t - p_t^{\rm J,v})\,, \tag{13}$$

with

$$R_{\rm NLL}(L) = -Lg_1(\alpha_s L) - g_2(\alpha_s L),$$
$$R_{\rm NNLL}(L) = R_{\rm NLL}(L) - \frac{\alpha_s}{\pi}g_3(\alpha_s L)\,, \tag{14}$$

and

$$R'_{\rm N(N)LL}(k_t) \equiv \frac{dR_{\rm N(N)LL}(\ln(Q/k_t))}{d\,\ln(Q/k_t)}\,. \tag{15}$$

The g_i functions read

$$g_1(\alpha_s L) = \frac{A^{(1)}}{\pi\beta_0}\frac{2\lambda + \ln(1-2\lambda)}{2\lambda}\,, \tag{16a}$$

$$g_2(\alpha_s L) = \frac{1}{2\pi\beta_0}\ln(1-2\lambda)\left(A^{(1)}\ln\frac{m_{\rm H}^2}{Q^2} + B^{(1)}\right) - \frac{A^{(2)}}{4\pi^2\beta_0^2}\frac{2\lambda + (1-2\lambda)\ln(1-2\lambda)}{1-2\lambda}$$
$$+ A^{(1)}\left(-\frac{\beta_1}{4\pi\beta_0^3}\frac{\ln(1-2\lambda)((2\lambda-1)\ln(1-2\lambda) - 2) - 4\lambda}{1-2\lambda} - \frac{1}{2\pi\beta_0}\frac{(2\lambda(1-\ln(1-2\lambda)) + \ln(1-2\lambda))}{1-2\lambda}\ln\frac{\mu_{\rm R}^2}{Q^2}\right)\,, \tag{16b}$$

$$g_3(\alpha_s L) = \left(A^{(1)}\ln\frac{m_{\rm H}^2}{Q^2} + B^{(1)}\right)\left(-\frac{\lambda}{1-2\lambda}\ln\frac{\mu_{\rm R}^2}{Q^2} + \frac{\beta_1}{2\beta_0^2}\frac{2\lambda + \ln(1-2\lambda)}{1-2\lambda}\right) - \frac{1}{2\pi\beta_0}\frac{\lambda}{1-2\lambda}\left(A^{(2)}\ln\frac{m_{\rm H}^2}{Q^2} + B^{(2)}\right)$$
$$- \frac{A^{(3)}}{4\pi^2\beta_0^2}\frac{\lambda^2}{(1-2\lambda)^2} + A^{(2)}\left(\frac{\beta_1}{4\pi\beta_0^3}\frac{2\lambda(3\lambda-1) + (4\lambda-1)\ln(1-2\lambda)}{(1-2\lambda)^2} - \frac{1}{\pi\beta_0}\frac{\lambda^2}{(1-2\lambda)^2}\ln\frac{\mu_{\rm R}^2}{Q^2}\right)$$
$$+ A^{(1)}\left(\frac{\lambda\left(\beta_0\beta_2(1-3\lambda) + \beta_1^2\lambda\right)}{\beta_0^4(1-2\lambda)^2} + \frac{(1-2\lambda)\ln(1-2\lambda)\left(\beta_0\beta_2(1-2\lambda) + 2\beta_1^2\lambda\right)}{2\beta_0^4(1-2\lambda)^2} + \frac{\beta_1^2}{4\beta_0^4}\frac{(1-4\lambda)\ln^2(1-2\lambda)}{(1-2\lambda)^2}\right.$$
$$\left. - \frac{\lambda^2}{(1-2\lambda)^2}\ln^2\frac{\mu_{\rm R}^2}{Q^2} - \frac{\beta_1}{2\beta_0^2}\frac{(2\lambda(1-2\lambda) + (1-4\lambda)\ln(1-2\lambda))}{(1-2\lambda)^2}\ln\frac{\mu_{\rm R}^2}{Q^2}\right)\,. \tag{16c}$$

The coefficients of the QCD beta function up to three loops read

$$\beta_0 = \frac{11C_A - 2n_f}{12\pi}\,, \qquad \beta_1 = \frac{17C_A^2 - 5C_A n_f - 3C_F n_f}{24\pi^2}\,,$$
$$\beta_2 = \frac{2857C_A^3 + (54C_F^2 - 615C_F C_A - 1415C_A^2)n_f + (66C_F + 79C_A)n_f^2}{3456\pi^3}\,, \tag{17}$$

and, for Higgs-boson production in gluon fusion, the coefficients $A^{(i)}$ and $B^{(i)}$ entering the above formulae are [72,73] (in units of $\alpha_s/(2\pi)$)

$$
\begin{aligned}
A^{(1)} &= 2C_A, \\
A^{(2)} &= \left(\frac{67}{9} - \frac{\pi^2}{3}\right)C_A^2 - \frac{10}{9}C_A n_f, \\
A^{(3)} &= \left(-22\zeta_3 - \frac{67\pi^2}{27} + \frac{11\pi^4}{90} + \frac{15503}{324}\right)C_A^3 + \left(\frac{10\pi^2}{27} - \frac{2051}{162}\right)C_A^2 n_f \\
&\quad + \left(4\zeta_3 - \frac{55}{12}\right)C_A C_F n_f + \frac{50}{81}C_A n_f^2, \\
B^{(1)} &= -\frac{11}{3}C_A + \frac{2}{3}n_f, \\
B^{(2)} &= \left(\frac{11\zeta_2}{6} - 6\zeta_3 - \frac{16}{3}\right)C_A^2 + \left(\frac{4}{3} - \frac{\zeta_2}{3}\right)C_A n_f + n_f C_F\,.
\end{aligned}
\tag{18}
$$

We finally report the expressions for the collinear coefficient function $C(\alpha_s(\mu))$ and the hard-virtual term $\mathcal{H}(\mu)$ in eq. (12) of the main text:

$$
C_{ij}(z, \alpha_s(\mu)) = \delta(1-z)\delta_{ij} + \frac{\alpha_s(\mu)}{2\pi}C_{ij}^{(1)}(z) + \mathcal{O}(\alpha_s^2)\,,
\tag{19}
$$

$$
\mathcal{H}(\mu) = 1 + \frac{\alpha_s(\mu)}{2\pi}\mathcal{H}^{(1)} + \mathcal{O}(\alpha_s^2)\,,
\tag{20}
$$

where

$$
C_{ij}^{(1)}(z) = -P_{ij}^{(0),\epsilon}(z) - \delta_{ij}\delta(1-z)C_A\frac{\pi^2}{12} + P_{ij}^{(0)}(z)\ln\frac{Q^2}{\mu_{\mathrm{F}}^2}\,,
\tag{21}
$$

$$
\mathcal{H}^{(1)} = H^{(1)} - \left(B^{(1)} + \frac{A^{(1)}}{2}\ln\frac{m_{\mathrm{H}}^2}{Q^2}\right)\ln\frac{m_{\mathrm{H}}^2}{Q^2} + \mathrm{d}_B\,2\pi\beta_0\ln\frac{\mu_{\mathrm{R}}^2}{m_{\mathrm{H}}^2}\,.
\tag{22}
$$

Here d_B is the α_s power of the LO cross section ($\mathrm{d}_B = 2$ for Higgs production). The coefficient $H^{(1)}$ encodes the pure hard virtual correction to the leading-order process $gg \to H$, and in the $\overline{\mathrm{MS}}$ scheme it is given by

$$
H^{(1)} = C_A\left(5 + \frac{7}{6}\pi^2\right) - 3C_F\,.
\tag{23}
$$

$P_{ij}^{(0),\epsilon}(z)$ is the $\mathcal{O}(\epsilon)$ term of the LO splitting function $P_{ij}^{(0)}(z)$:

$$
P_{qq}^{(0),\epsilon}(z) = -C_F(1-z)\,,
\tag{24a}
$$

$$
P_{gq}^{(0),\epsilon}(z) = -C_F z\,,
\tag{24b}
$$

$$
P_{qg}^{(0),\epsilon}(z) = -z(1-z)\,,
\tag{24c}
$$

$$
P_{gg}^{(0),\epsilon}(z) = 0\,.
\tag{24d}
$$

The anomalous dimensions $\mathbf{\Gamma}_{\nu_\ell}$ and $\mathbf{\Gamma}_{\nu_\ell}^{(C)}$ in eq. (12) of the main text are defined as

$$
[\mathbf{\Gamma}_{\nu_\ell}(\alpha_s(\mu))]_{ij} = \frac{\alpha_s(\mu)}{\pi}\int_0^1 dz\, z^{\nu_\ell - 1}\hat{P}_{ij}(z, \alpha_s(\mu))\,,
\tag{25}
$$

$$
[\mathbf{\Gamma}_{\nu_\ell}^{(C)}(\alpha_s(\mu))]_{ij} = 2\beta(\alpha_s(\mu))\frac{d\ln C_{\nu_\ell,ij}(\alpha_s(\mu))}{d\alpha_s(\mu)}\,,
\tag{26}
$$

where

$$
C_{\nu_\ell,ij}(\alpha_s(\mu)) \equiv \int_0^1 dz\, z^{\nu_\ell - 1}C_{ij}(z, \alpha_s(\mu))\,,
\tag{27}
$$

and $\hat{P}_{ij}$ is the perturbative expansion of the regularised splitting function (see e.g. ref. [74]). Finally, we report the explicit formulae for the clustering (10) and correlated (11) corrections used in the main result of the letter. We find

$$
\begin{aligned}
\mathcal{F}_{\text{clust}} = &\frac{1}{2!} \int_0^\infty \frac{dk_{t,a}}{k_{t,a}} \frac{dk_{t,b}}{k_{t,b}} \int_{-\infty}^\infty d\Delta\eta_{ab} \int_{-\pi}^\pi \frac{d\Delta\phi_{ab}}{2\pi} \left(2C_A \frac{\alpha_s(k_{t,b})}{\pi} \right) \left(4C_A \frac{\alpha_s(k_{t,a})}{\pi} \ln \frac{m_{\text{H}}}{k_{t,a}} \right) J_{ab}(R) \\
&\times \left[\Theta\left(p_t^{\text{J,v}} - |\vec{k}_{t,a} + \vec{k}_{t,b}| \right) - \Theta\left(p_t^{\text{J,v}} - \max\{k_{t,a}, k_{t,b}\} \right) \right] e^{i\vec{b}\cdot\vec{k}_{t,a}} e^{i\vec{b}\cdot\vec{k}_{t,b}} \\
= &\frac{1}{2!} \int_0^\infty \frac{dk_{t,a}}{k_{t,a}} \frac{dk_{t,b}}{k_{t,b}} \int_{-\infty}^\infty d\Delta\eta_{ab} \int_{-\pi}^\pi \frac{d\Delta\phi_{ab}}{2\pi} 8\, C_A^2 \frac{\alpha_s^2}{\pi^2} \frac{\ln(Q/k_{t,a})}{(1 - 2\beta_0\alpha_s \ln(Q/k_{t,a}))^2} J_{ab}(R) \\
&\times \left[\Theta\left(p_t^{\text{J,v}} - |\vec{k}_{t,a} + \vec{k}_{t,b}| \right) - \Theta\left(p_t^{\text{J,v}} - \max\{k_{t,a}, k_{t,b}\} \right) \right] e^{i\vec{b}\cdot\vec{k}_{t,a}} e^{i\vec{b}\cdot\vec{k}_{t,b}} + \mathcal{O}(\text{N}^3\text{LL}) \,,
\end{aligned}
\tag{28}
$$

where in the last step we have introduced the resummation scale Q and neglected corrections beyond NNLL. Similarly, within the same approximation, for the correlated corrections we find

$$
\begin{aligned}
\mathcal{F}_{\text{correl}} = &\frac{1}{2!} \int_0^\infty \frac{dk_{t,a}}{k_{t,a}} \frac{dk_{t,b}}{k_{t,b}} \int_{-\infty}^\infty d\Delta\eta_{ab} \int_{-\pi}^\pi \frac{d\Delta\phi_{ab}}{2\pi} 8\, C_A^2 \frac{\alpha_s^2}{\pi^2} \frac{\ln(Q/k_{t,a})}{(1 - 2\beta_0\alpha_s \ln(Q/k_{t,a}))^2} \left(1 - J_{ab}(R) \right) \\
&\times \mathcal{C}\left(\Delta\eta_{ab}, \Delta\phi_{ab}, \frac{k_{t,a}}{k_{t,b}} \right) \left[\Theta\left(p_t^{\text{J,v}} - \max\{k_{t,a}, k_{t,b}\} \right) - \Theta\left(p_t^{\text{J,v}} - |\vec{k}_{t,a} + \vec{k}_{t,b}| \right) \right] e^{i\vec{b}\cdot\vec{k}_{t,a}} e^{i\vec{b}\cdot\vec{k}_{t,b}} \,.
\end{aligned}
\tag{29}
$$

The function $\mathcal{C}$ is defined as the ratio of the correlated part of the double-soft squared amplitude to the product of the two single-soft squared amplitudes, namely

$$
\mathcal{C}\left(\Delta\eta_{ab}, \Delta\phi_{ab}, \frac{k_{t,a}}{k_{t,b}} \right) \equiv \frac{\tilde{M}^2(k_a, k_b)}{M^2(k_a)\, M^2(k_b)} \,.
\tag{30}
$$

Adopting the parametrisation of ref. [57] for the amplitudes, we have

$$
M^2(k) = 2\, C\, W(k) \,, \quad \tilde{M}^2(k_a, k_b) = C\, C_A(2S + H_{\text{g}}) + C\, n_f H_{\text{q}} \,,
\tag{31}
$$

where $W(k) \equiv 2/k_t^2$, and $C = C_A$ for Higgs production. The functions S, H_{g}, and H_{q} are given in eqs. (2.4)-(2.6) of ref. [57]. We point out that the symmetry factor $1/2!$ in eq. (29) accounts for the contribution from two identical gluons. Conversely, the contribution describing the emission of a $q\bar{q}$ pair in the squared amplitude encodes an extra factor of 2 that cancels against the symmetry factor in this case.

We conclude this section by observing that all of the above integrals have a Landau singularity that must be regulated with some non-perturbative procedure. Given that the divergence occurs at very small values of the transverse momentum (much below $1\,\text{GeV}$), it does not affect the region of phenomenological relevance considered in our results. Therefore, in our study, we simply set the result to zero at the singularity and below.

2. Momentum-space formulation and implementation in RadISH

The momentum-space formulation of refs. [28,29] allows a more differential description of the radiation with respect to the impact-parameter-space formulation used in the letter. The access to differential information comes at the cost of less compact equations, that however can be efficiently evaluated through a Monte Carlo method. The versatility of the Monte Carlo implementation can be exploited observing that the resummation for the two considered observables (p_t^{H} and p_t^{J}) features the same momentum-space radiator $R_{\text{N(N)LL}}$. As a result, the joint resummation can be achieved by modifying the phase-space constraint with respect to the inclusive p_t^{H} result of ref. [28], and by adding the clustering and correlated corrections discussed in the main text.

The resummation is more easily formulated at the level of the double-cumulative distribution, namely

$$
\sigma(p_t^{\text{J,v}}, p_t^{\text{H,v}}) \equiv \int_0^{p_t^{\text{H,v}}} dp_t^{\text{H}} \int_0^{p_t^{\text{J,v}}} dp_t^{\text{J}} \frac{d\sigma}{dp_t^{\text{H}} dp_t^{\text{J}}} \,,
\tag{32}
$$

and in the following we report both the NLL and the NNLL results in turn.

a. NLL formula

At NLL, the measurement function for the pair of observables under consideration for a state with n emissions reads

$$\Theta(p_t^{\text{J,v}} - \max\{k_{t,1}, \ldots, k_{t,n}\})\Theta(p_t^{\text{H,v}} - |\vec{k}_{t,1} + \cdots + \vec{k}_{t,n}|). \tag{33}$$

Following ref. [28], we single out the emission with the largest transverse momentum $k_{t,1}$, and express the NLL cross section as

$$\sigma^{\text{NLL}}(p_t^{\text{J,v}}, p_t^{\text{H,v}}) = \int_0^{p_t^{\text{J,v}}} \frac{dk_{t,1}}{k_{t,1}} \frac{d\phi_1}{2\pi} \int d\mathcal{Z} \frac{d}{dL_{t,1}} \left[-e^{-R_{\text{NLL}}(L_{t,1})} \mathcal{L}_{\text{NLL}}(\mu_{\text{F}} e^{-L_{t,1}}) \right] \Theta\left(p_t^{\text{H,v}} - |\vec{k}_{t,1} + \cdots + \vec{k}_{t,n+1}| \right), \tag{34}$$

where $L_{t,1} \equiv \ln(Q/k_{t,1})$, and the factor $\mathcal{L}_{\text{NLL}}$ reads

$$\mathcal{L}_{\text{NLL}}(\mu) \equiv M_{\text{gg} \to \text{H}}^2 f_g(\mu, x_1) f_g(\mu, x_2), \tag{35}$$

where we introduced the explicit x dependence of the parton densities for later convenience. We also introduced the measure $d\mathcal{Z}$ defined as

$$\int d\mathcal{Z} \equiv \epsilon^{\hat{R}'(k_{t,1})} \sum_{n=0}^{\infty} \frac{1}{n!} \prod_{i=2}^{n+1} \int_{\epsilon k_{t,1}}^{k_{t,1}} \frac{dk_{t,i}}{k_{t,i}} \frac{d\phi_i}{2\pi} \hat{R}'(k_{t,1}), \tag{36}$$

with $\epsilon \ll 1$ an infrared, constant, resolution parameter that allows for a numerical evaluation of eq. (34) in four space-time dimensions. We stress that the dependence on ϵ entirely cancels in eq. (34) for sufficiently small values: in practice we set $\epsilon = e^{-20}$. We also introduced the quantity [28]

$$\hat{R}'(k_{t,1}) \equiv -\frac{d}{dL_{t,1}}(L_{t,1} g_1(\alpha_s L_{t,1})) = 4C_A \frac{\alpha_s}{\pi} \frac{L_{t,1}}{(1 - 2\beta_0 \alpha_s L_{t,1})}. \tag{37}$$

b. NNLL formula

Following the discussion at NLL, a first contribution to the NNLL cross section is given by the NNLL formula for inclusive p_t^{H}, supplemented by the jet-veto constraint. This reads [28]

$$\sigma_{\text{incl}}^{\text{NNLL}}(p_t^{\text{J,v}}, p_t^{\text{H,v}}) = \int_0^{p_t^{\text{J,v}}} \frac{dk_{t,1}}{k_{t,1}} \frac{d\phi_1}{2\pi} \int d\mathcal{Z} \left\{ \frac{d}{dL_{t,1}} \left[-e^{-R_{\text{NNLL}}(L_{t,1})} \mathcal{L}_{\text{NNLL}}\left(\mu_{\text{F}} e^{-L_{t,1}} \right) \right] \Theta\left(p_t^{\text{H,v}} - |\vec{k}_{t,1} + \cdots + \vec{k}_{t,n+1}| \right) \right.$$

$$+ e^{-R_{\text{NLL}}(L_{t,1})} \hat{R}'(k_{t,1}) \int_0^{k_{t,1}} \frac{dk_{t,s_1}}{k_{t,s_1}} \frac{d\phi_{s_1}}{2\pi} \left[\left(\delta\hat{R}'(k_{t,1}) + \hat{R}''(k_{t,1}) \ln \frac{k_{t,1}}{k_{t,s_1}} \right) \mathcal{L}_{\text{NLL}}\left(\mu_{\text{F}} e^{-L_{t,1}} \right) - \frac{d}{dL_{t,1}} \mathcal{L}_{\text{NLL}}\left(\mu_{\text{F}} e^{-L_{t,1}} \right) \right]$$

$$\times \left. \left[\Theta\left(p_t^{\text{H,v}} - |\vec{k}_{t,1} + \cdots + \vec{k}_{t,n+1} + \vec{k}_{t,s_1}| \right) - \Theta\left(p_t^{\text{H,v}} - |\vec{k}_{t,1} + \cdots + \vec{k}_{t,n+1}| \right) \right] \right\}, \tag{38}$$

where $\mathcal{L}_{\text{NNLL}}$ is given by

$$\mathcal{L}_{\text{NNLL}}(\mu) \equiv M_{\text{gg} \to \text{H}}^2 \left[f_g(\mu, x_1) f_g(\mu, x_2) \left(1 + \frac{\alpha_s}{2\pi} \mathcal{H}^{(1)} \right) + \right.$$

$$\left. + \frac{\alpha_s}{2\pi} \frac{1}{1 - 2\alpha_s \beta_0 L_{t,1}} \sum_k \left(\int_{x_1}^1 \frac{dz}{z} C_{gk}^{(1)}(z) f_k\left(\mu, \frac{x_1}{z} \right) f_g(\mu, x_2) + \{x_1 \leftrightarrow x_2\} \right) \right]. \tag{39}$$

Finally, we introduced

$$\delta\hat{R}'(k_{t,1}) \equiv -\frac{d\, g_2(\alpha_s L_{t,1})}{dL_{t,1}}, \tag{40}$$

$$\hat{R}''(k_{t,1}) \equiv \frac{d\, \hat{R}'(k_{t,1})}{dL_{t,1}}. \tag{41}$$

When considering $\sigma_{\text{incl}}^{\text{NNLL}}(p_t^{\text{J,v}}, p_t^{\text{H,v}})$ we used the phase-space constraint of eq. (33). As discussed in the letter, this measurement function assumes that the emissions are widely separated in rapidity and therefore do not get clustered by the jet algorithm. However, at NNLL at most two soft emissions are allowed to get arbitrarily close in angle and to get clustered into the same jet. Accounting for this type of configurations led to the formulation of the clustering ($\mathcal{F}_{\text{clust}}$) and correlated ($\mathcal{F}_{\text{correl}}$) corrections in the main text. In the following we will formulate these two corrections directly in momentum space.

The clustering correction can be expressed as

$$\sigma_{\text{clust}}^{\text{NNLL}}(p_t^{\text{J,v}}, p_t^{\text{H,v}}) = \int_0^\infty \frac{dk_{t,1}}{k_{t,1}} \frac{d\phi_1}{2\pi} \int d\mathcal{Z}\, e^{-R_{\text{NLL}}(L_{t,1})}\, \mathcal{L}_{\text{NLL}}\left(\mu_{\text{F}} e^{-L_{t,1}}\right) 8\, C_A^2 \frac{\alpha_s^2}{\pi^2} \frac{L_{t,1}}{(1 - 2\beta_0 \alpha_s L_{t,1})^2}\, \Theta\left(p_t^{\text{J,v}} - \max_{i>1}\{k_{t,i}\}\right)$$

$$\times \left\{ \int_0^{k_{t,1}} \frac{dk_{t,s_1}}{k_{t,s_1}} \frac{d\phi_{s_1}}{2\pi} \int_{-\infty}^\infty d\Delta\eta_{1s_1}\, J_{1s_1}(R) \left[\Theta\left(p_t^{\text{J,v}} - |\vec{k}_{t,1} + \vec{k}_{t,s_1}|\right) - \Theta\left(p_t^{\text{J,v}} - k_{t,1}\right) \right] \Theta\left(p_t^{\text{H,v}} - |\vec{k}_{t,1} + \cdots + \vec{k}_{t,n+1} + \vec{k}_{t,s_1}|\right) \right.$$

$$+ \frac{1}{2!} \hat{R}'(k_{t,1}) \int_0^{k_{t,1}} \frac{dk_{t,s_1}}{k_{t,s_1}} \frac{dk_{t,s_2}}{k_{t,s_2}} \frac{d\phi_{s_1}}{2\pi} \frac{d\phi_{s_2}}{2\pi} \int_{-\infty}^\infty d\Delta\eta_{s_1 s_2}\, J_{s_1 s_2}(R) \left[\Theta\left(p_t^{\text{J,v}} - |\vec{k}_{t,s_1} + \vec{k}_{t,s_2}|\right) - \Theta\left(p_t^{\text{J,v}} - \max\{k_{t,s_1}, k_{t,s_2}\}\right) \right]$$

$$\left. \times \Theta\left(p_t^{\text{H,v}} - |\vec{k}_{t,1} + \cdots + \vec{k}_{t,n+1} + \vec{k}_{t,s_1} + \vec{k}_{t,s_2}|\right) \Theta\left(p_t^{\text{J,v}} - k_{t,1}\right) \right\}, \tag{42}$$

where we have explicitly separated the configuration in which one of the two clustered emissions is the hardest (k_1), from the configuration in which both clustered emissions have $k_{t,s_1/s_2} \leq k_{t,1}$. Although the latter step is not necessary, we find it convenient to keep the two contributions separate for a Monte Carlo implementation. The same arguments can be applied to the correlated correction, which can be expressed as

$$\sigma_{\text{correl}}^{\text{NNLL}}(p_t^{\text{J,v}}, p_t^{\text{H,v}}) = \int_0^\infty \frac{dk_{t,1}}{k_{t,1}} \frac{d\phi_1}{2\pi} \int d\mathcal{Z}\, e^{-R_{\text{NLL}}(L_{t,1})}\, \mathcal{L}_{\text{NLL}}\left(\mu_{\text{F}} e^{-L_{t,1}}\right) 8\, C_A^2 \frac{\alpha_s^2}{\pi^2} \frac{L_{t,1}}{(1 - 2\beta_0 \alpha_s L_{t,1})^2}\, \Theta\left(p_t^{\text{J,v}} - \max_{i>1}\{k_{t,i}\}\right)$$

$$\times \left\{ \int_0^{k_{t,1}} \frac{dk_{t,s_1}}{k_{t,s_1}} \frac{d\phi_{s_1}}{2\pi} \int_{-\infty}^\infty d\Delta\eta_{1s_1}\, \mathcal{C}\left(\Delta\eta_{1s_1}, \Delta\phi_{1s_1}, \frac{k_{t,1}}{k_{t,s_1}}\right) (1 - J_{1s_1}(R)) \right.$$

$$\times \left[\Theta\left(p_t^{\text{J,v}} - k_{t,1}\right) - \Theta\left(p_t^{\text{J,v}} - |\vec{k}_{t,1} + \vec{k}_{t,s_1}|\right) \right] \Theta\left(p_t^{\text{H,v}} - |\vec{k}_{t,1} + \cdots + \vec{k}_{t,n+1} + \vec{k}_{t,s_1}|\right)$$

$$+ \frac{1}{2!} \hat{R}'(k_{t,1}) \int_0^{k_{t,1}} \frac{dk_{t,s_1}}{k_{t,s_1}} \frac{dk_{t,s_2}}{k_{t,s_2}} \frac{d\phi_{s_1}}{2\pi} \frac{d\phi_{s_2}}{2\pi} \int_{-\infty}^\infty d\Delta\eta_{s_1 s_2}\, \mathcal{C}\left(\Delta\eta_{s_1 s_2}, \Delta\phi_{s_1 s_2}, \frac{k_{t,s_2}}{k_{t,s_1}}\right) (1 - J_{s_1 s_2}(R))\, \Theta\left(p_t^{\text{J,v}} - k_{t,1}\right)$$

$$\left. \times \left[\Theta\left(p_t^{\text{J,v}} - \max\{k_{t,s_1}, k_{t,s_2}\}\right) - \Theta\left(p_t^{\text{J,v}} - |\vec{k}_{t,s_1} + \vec{k}_{t,s_2}|\right) \right] \Theta\left(p_t^{\text{H,v}} - |\vec{k}_{t,1} + \cdots + \vec{k}_{t,n+1} + \vec{k}_{t,s_1} + \vec{k}_{t,s_2}|\right) \right\}. \tag{43}$$

The NNLL double-cumulative distribution is then obtained by summing the three contributions, namely

$$\sigma^{\text{NNLL}}(p_t^{\text{J,v}}, p_t^{\text{H,v}}) = \sigma_{\text{incl}}^{\text{NNLL}}(p_t^{\text{J,v}}, p_t^{\text{H,v}}) + \sigma_{\text{clust}}^{\text{NNLL}}(p_t^{\text{J,v}}, p_t^{\text{H,v}}) + \sigma_{\text{correl}}^{\text{NNLL}}(p_t^{\text{J,v}}, p_t^{\text{H,v}}). \tag{44}$$

We refer to Section 4.3 of ref. [29] for the Monte Carlo evaluation of the above equations, and to Section 4.2 of the same article for the procedure used to expand them at a fixed perturbative order.

3. Asymptotic limits of the joint-resummation formula

In this section we perform the asymptotic limits of eq. (12) of the main text, and verify that it reproduces the NNLL results for p_t^{H} and jet-veto resummation, respectively. We start by taking the limit $p_t^{\text{J,v}} \sim m_{\text{H}} \gg p_t^{\text{H}}$. Using the fact that

$$S_{\text{NNLL}} \underset{p_t^{\text{J,v}} \sim m_{\text{H}} \gg p_t^{\text{H}}}{\sim} R_{\text{NNLL}}(L), \tag{45}$$

and observing that eqs. (28), (29) vanish since both Θ functions are satisfied, we obtain

$$\frac{d\sigma(p_t^{\text{J,v}})}{dy^{\text{H}} d^2\vec{p}_t^{\text{H}}} \simeq M_{\text{gg} \to \text{H}}^2\, \mathcal{H}(\alpha_s(m_{\text{H}})) \int_{\mathcal{C}_1} \frac{d\nu_1}{2\pi i} \int_{\mathcal{C}_2} \frac{d\nu_2}{2\pi i} x_1^{-\nu_1} x_2^{-\nu_2} \int \frac{d^2\vec{b}}{4\pi^2} e^{-i\vec{b}\cdot\vec{p}_t^{\text{H}}}\, e^{-R_{\text{NNLL}}} \tag{46}$$

$$\times f_{\nu_1, a_1}(b_0/b)\, f_{\nu_2, a_2}(b_0/b) C_{\nu_1, ga_1}(\alpha_s(b_0/b))\, C_{\nu_2, ga_2}(\alpha_s(b_0/b)),$$

that, upon performing the Mellin integrals, coincides with the inclusive p_t^{H} resummation (see for instance ref. [25]).

Similarly, we now consider the limit $p_t^{\text{H}} \sim m_{\text{H}} \gg p_t^{\text{J,v}}$. This limit corresponds to taking the impact parameter b to zero while keeping $b\,p_t^{\text{H}}$ fixed. We observe that this limit probes the region in which the approximation (7) of the main text cannot be made. This issue is commonly circumvented by modifying the b-space logarithms as in [25]. Alternatively, one can avoid making the approximation (7) in the first place, which guarantees the $b \to 0$ limit to be well defined. In this case one exploits the fact that

$$\lim_{b \to 0} J_0(bx) = 1 \,, \tag{47}$$

and obtains

$$
\begin{aligned}
\frac{d\sigma(p_t^{\text{J,v}})}{dy^{\text{H}} d^2\vec{p}_t^{\text{H}}} &\simeq M_{gg \to \text{H}}^2 \, \mathcal{H}(\alpha_s(m_{\text{H}})) \int_{\mathcal{C}_1} \frac{d\nu_1}{2\pi i} \int_{\mathcal{C}_2} \frac{d\nu_2}{2\pi i} x_1^{-\nu_1} \, x_2^{-\nu_2} \int \frac{d^2\vec{b}}{4\pi^2} e^{-i\vec{b}\cdot\vec{p}_t^{\text{H}}} \, e^{-S_{\text{NNLL}}} \left(1 + \mathcal{F}_{\text{clust}} + \mathcal{F}_{\text{correl}}\right) \\
&\times f_{\nu_1, a_1}(m_{\text{H}}) \, f_{\nu_2, a_2}(m_{\text{H}}) \left[\mathcal{P} \, e^{-\int_{p_t^{\text{J,v}}}^{m_{\text{H}}} \frac{d\mu}{\mu} \boldsymbol{\Gamma}_{\nu_1}(\alpha_s(\mu))}\right]_{c_1 a_1} \left[\mathcal{P} \, e^{-\int_{p_t^{\text{J,v}}}^{m_{\text{H}}} \frac{d\mu}{\mu} \boldsymbol{\Gamma}_{\nu_2}(\alpha_s(\mu))}\right]_{c_2 a_2} \\
&\times C_{\nu_1, g b_1}(\alpha_s(m_{\text{H}})) \, C_{\nu_2, g b_2}(\alpha_s(m_{\text{H}})) \left[\mathcal{P} \, e^{-\int_{p_t^{\text{J,v}}}^{m_{\text{H}}} \frac{d\mu}{\mu} \boldsymbol{\Gamma}_{\nu_1}^{(C)}(\alpha_s(\mu))}\right]_{c_1 b_1} \left[\mathcal{P} \, e^{-\int_{p_t^{\text{J,v}}}^{m_{\text{H}}} \frac{d\mu}{\mu} \boldsymbol{\Gamma}_{\nu_2}^{(C)}(\alpha_s(\mu))}\right]_{c_2 b_2} \\
&= M_{gg \to \text{H}}^2 \, \mathcal{H}(\alpha_s(m_{\text{H}})) \int_{\mathcal{C}_1} \frac{d\nu_1}{2\pi i} \int_{\mathcal{C}_2} \frac{d\nu_2}{2\pi i} x_1^{-\nu_1} \, x_2^{-\nu_2} \int \frac{d^2\vec{b}}{4\pi^2} e^{-i\vec{b}\cdot\vec{p}_t^{\text{H}}} \, e^{-S_{\text{NNLL}}} \left(1 + \mathcal{F}_{\text{clust}} + \mathcal{F}_{\text{correl}}\right) \\
&\times f_{\nu_1, a_1}(p_t^{\text{J,v}}) \, f_{\nu_2, a_2}(p_t^{\text{J,v}}) C_{\nu_1, g a_1}(\alpha_s(p_t^{\text{J,v}})) \, C_{\nu_2, g a_2}(\alpha_s(p_t^{\text{J,v}})) \,,
\end{aligned}
\tag{48}
$$

where in the second line we applied the evolution operators from m_{H} to $p_t^{\text{J,v}}$ to the parton densities and coefficient functions. Finally, by observing that

$$S_{\text{NNLL}} \underset{p_t^{\text{H}} \sim m_{\text{H}} \gg p_t^{\text{J,v}}}{\sim} R_{\text{NNLL}}(\ln(m_{\text{H}}/p_t^{\text{J,v}})) \,, \tag{49}$$

the integral over the impact parameter b becomes trivial

$$\int \frac{d^2\vec{b}}{4\pi^2} e^{-i\vec{b}\cdot\vec{p}_t^{\text{H}}} = \delta^2(\vec{p}_t^{\text{H}}) \,. \tag{50}$$

As a consequence, upon integration over $\vec{p}_t^{\text{H}}$, eq. (48) yields

$$
\begin{aligned}
\frac{d\sigma(p_t^{\text{J,v}})}{dy^{\text{H}}} &= M_{gg \to \text{H}}^2 \, \mathcal{H}(\alpha_s(m_{\text{H}})) \, e^{-R_{\text{NNLL}}(\ln(m_{\text{H}}/p_t^{\text{J,v}}))} \left(1 + \mathcal{F}_{\text{clust}} + \mathcal{F}_{\text{correl}}\right) \\
&\times \left[f(p_t^{\text{J,v}}) \otimes C(\alpha_s(p_t^{\text{J,v}}))\right]_g (x_1) \left[f(p_t^{\text{J,v}}) \otimes C(\alpha_s(p_t^{\text{J,v}}))\right]_g (x_2) \,,
\end{aligned}
\tag{51}
$$

that coincides with the standard jet-veto resummation [34] differential in the Higgs-boson rapidity, where the convolution between two functions $f(x)$ and $g(x)$ is defined as

$$[f \otimes g](x) \equiv \int_x^1 \frac{dz}{z} f(z) g\left(\frac{x}{z}\right) \,. \tag{52}$$